Marine Pollution Bulletin 157 (2020) 111375

Contents lists available at ScienceDirect

Marine Pollution Bulletin

journal homepage: www.elsevier.com/locate/marpolbul

Ecotoxic response of nematodes to ivermectin, a potential anti-COVID-19 drug treatment

Naceur Essid[a], Mohamed Allouche[a], Mounira Lazzem[a], Abdel Halim Harrath[b], Lamjed Mansour[b], Saleh Alwasel[b], Ezzeddine Mahmoudi[a], Hamouda Beyrem[a], Fehmi Boufahja[a,*]

[a] University of Carthage, Faculty of Sciences of Bizerte, Laboratory of Environment Biomonitoring, Coastal Ecology and Ecotoxicology Unit, 7021 Zarzouna, Tunisia
[b] King Saud University, Zoology Department, College of Science, Box 2455, Riyadh 11451, Saudi Arabia

ARTICLE INFO

Keywords:
COVID-19
Ivermectin
Ecotoxicity
Meiobenthic nematodes

ABSTRACT

At the end of March 2020, ivermectin was confirmed as a drug for COVID-19 treatment. A significant amount of ivermectin could deposit into sediments of the semi-closed Mediterranean Sea, where three European COVID-19 epicenters are located: Italy, Spain, and France. Meiobenthic nematodes were exposed to three ivermectin doses (1.8 ng.g^{-1}, 9 ng.g^{-1}, and 18 ng.g^{-1}) for 10 days. Ivermectin caused a great reduction in abundance. However, the diversity indices decreased only at high doses. Ivermectin disadvantaged the 1B-Cr-Id functional type (non-selective deposit feeders and nematodes with circular or indistinct amphids) and benefited the 2A-REL-Sp type (epistrate feeders and nematodes with rounded or elongated loop amphids). Thus, Trophic Diversity and Amphideal Diversity index values increased with sedimentary ivermectin enrichment. Large amphideal foveas were more efficient for 2A-REL-Sp nematodes to avoid ivermectin. The responses of the functional type 2A-REL-Sp and corresponding taxa predict post-COVID-19 environmental concerns and the bioaccumulation of ivermectin in seafoods.

1. Introduction

Coronavirus Infectious Disease 2019 (COVID-19) is an emerging viral global crisis caused by the SARS-CoV-2 coronavirus strain (Whitworth, 2020). Worldwide, the number of people affected by the virus (3,578,301, https://www.who.int/, visited on May 5, 2020) has almost tripled in the last 12 days , as has the number of deaths. The overall case fatality rate (i.e., the number of deaths out of total number of infected persons) is 7% with rates from 10 to 20% in the main European epicenters: France, the United Kingdom, Italy, and Spain. Outside of Mediterranea, the United States of America leads the world in the number of infected cases, which are approaching a million, and a fatality rate of 5.66% while struggling to curtail the virus.

Since the beginning of the COVID-19 pandemic, the scientific community has circulated the following as potential treatments (Abd El-Aziz and Stockand, 2020): (1) chloroquine, a treatment originally intended for the prevention and treatment of malaria which is a parasitic (nonviral); (2) several antivirals that were previously used to stop other viruses (e.g., HIV, dengue, influenza, and Zika) from replicating, at least in laboratory conditions; (3) the use of vaccines to reduce the impact of COVID-19 such the tuberculosis vaccination, which treats a bacterial (nonviral) disease, and (4) the use of antibody serums which requires injecting the blood plasma serum of recovered patients into the blood of critically ill patients and is commonly called “serotherapy.” The common theme of all these treatments (except antivirals) is to suppress the action of COVID-19 by stimulating the immune system.

A recent study by Caly et al. (2020), Australian scientists from Monash University and the Peter Doherty Institute for Infection and Immunity, suggests that ivermectin is able to produce a ~5000-fold reduction in viral RNA and stop SARS-CoV-2 from replicating within 24 to 48 h after cell culture exposure. Since the 1980s, ivermectin has been used as an antiparasitic to treat and prevent diseases related to invertebrate parasites in humans, pets, and livestock (Mesa et al., 2020). The use of ivermectin as a possible treatment for COVID-19 has had promising results in laboratory studies and provided some promise, after urgent clinical tests on people infected with SARS-CoV-2, to enable precise doses and delivery methods which could stop the progress of the pandemic (Caly et al., 2020). If the efficacy of this drug is clinically accepted for use against COVID-19, which is likely to occur in the very near future based on enormous global efforts in terms of means and money, the release of ivermectin into marine areas will increase suddenly which poses many questions concerning its short-term and

* Corresponding author.
E-mail address: fehmiboufahja@yahoo.fr (F. Boufahja).

https://doi.org/10.1016/j.marpolbul.2020.111375
Received 5 May 2020; Accepted 10 June 2020
Available online 11 June 2020
0025-326X/

long-term ecotoxicity.

To investigate short-term ecotoxicity, the following criteria were needed: (1) experiments with short durations to quickly evaluate drug which could be used in significant quantities by COVID-19 patients around the world; (2) small model organisms at the base of the food chain to detect toxic effects in early stages of drug distribution; (3) a benthic model taxa with no planktonic larvae, since ivermectin is persistent and adheres quickly to marine sediments with a half-life that exceeds 100 days (Halley et al., 1993; Davies et al., 1998); and (4) a model taxa with a global distribution to generalize conclusions for distant countries influenced by the COVID-19 pandemic. All these criteria are met in free-living marine nematodes which constitute the most abundant and diverse component of marine ecosystems (Moens and Vincx, 1997). They can reach densities of up to several million individuals m^{-2} (Moens and Vincx, 1997) and > 7000 species have been described (Bezerra et al., 2019). These holobenthic worms are small (1–5 mm in average length) with a significant role in the "small food web" which is made up of bacteria, protists, and meiofauna (Heip et al., 1985). Schratzberger and Warwick (1998), they have short generation times (egg to egg-laying parent) of days to weeks, and thus are suitable to set-up in short-term laboratory bioassays. Numerous studies have also highlighted the high potential of nematodes as bioindicators due to their susceptibility, resistance, or proliferation with respect to xenobiotic loads (Lee and Correa, 2005; Mahmoudi et al., 2005; Beyrem et al., 2007; Hedfi et al., 2007; Mahmoudi et al., 2007; Hermi et al., 2009; Beyrem et al., 2010). Interestingly, meiobenthic nematodes constitute the main food source for the larvae of several microbenthic taxa that are consumed by humans as seafood which include fishes (Albertini-Berhaut, 1974), crabs (Fitzhugh and Fleeger, 1985), and shrimps (Wilcox and Jeffries, 1979). Given these circumstances, we can anticipate that the consumption of seafoods captured from the coasts of countries where ivermectin was used to treat COVID-19 represents a major human health risk. Thus, it is important to identify "tolerant" and "opportunistic" nematodes as these taxa probably possess the ability to accumulate or metabolize ivermectin that is present in their environments.

At this point, the focus is on the results of an experimental study which aims to evaluate whether the eventual massive use of ivermectin against COVID-19 will lead to ecotoxic effects on meiobenthic nematodes, or not, after assessing their abundance and taxonomic and functional diversity in response to a range of ivermectin doses.

2. Materials and methods

2.1. Sampling

Samples consisting of the top 3 cm of sediment were collected from a pristine coastal site at Ghar El Melh lagoon (37°0910′N; 10°1301′E) (Fig. 1) using plexiglass hand-cores (3.6 cm inner diameter) (Coull and Chandler, 1992). On the sampling day, the following measurements were obtained: water depth of 40 cm, salinity of 38.2 PSU, pH of 8.35 and temperature of 16.8 °C.

2.2. Sediment characteristics

Upon returning to the laboratory, the sediment was manually homogenized with a large spatula. First, sub-samples were dried at 45 °C until constant weight to evaluate water content and then used after heating to 450 °C for 6 h to measure the percentage of organic matter (Fabiano and Danovaro, 1994). The silt-clay fraction (< 63 μm) was deduced after wet sieving dried sediment on 63 μm mesh size (Buchanan, 1971). Cumulative curves were also plotted for the coarse fraction (≥63 μm) to determine the mean grain size (Buchanan, 1971). Three sub-sample replicates, of 100 g Dry Weight (DW) each, were analyzed. The results showed that the sediment used at the start of the experiment was characterized by a mean grain size of 1.04 ± 0.07 mm, organic matter of 9.14 ± 1.76%, a water content of 26.77 ± 4.14%, composed of a coarse fraction of 43.52 ± 6.41%, and silt-clay fraction of 56.48 ± 6.41%.

2.3. Sediment contamination and experimental set-up

The sediment collected from the field was divided in two parts; the first portion was designated for experimental contamination and the second portion was stored in a bucket and aerated using an air pump. Before starting the contamination process, the sediment was defaunated by repeating a defaunation process, freezing the sediment to −20 °C for 12 h and thawing at room temperature for 48 h, three times (Schratzberger et al., 2004). Numerous sediment sub-samples of 100 g Wet Weight (WW) were used for invermectin contaminatation. After the ivermectin was dissolved in acetone (99.8%), and the sediment was spiked with the drug in a cold dark room at 4 °C to avoid any eventual transformation of the ivermectin. The work of Louati et al. (2013) and Allouche et al. (2020a) proved that acetone is not toxic to meiobenthic nematodes. After three days of acclimatization, the overlying water was removed from the buckets containing natural sediment. Then, 100 g WW of contaminated sediment were gently mixed with a large spatula with 200 g WW of sediment populated with meiofauna to reach three doses of ivermectin: D1 (1.8 $ng.g^{-1}$), D2 (9 $ng.g^{-1}$), and D3 (18 $ng.g^{-1}$). The doses were chosen based on the work of Davies et al. (1998) who provided a sediment dwelling taxon, the mud shrimp (*Corophium volutator*), with ivermectin and experienced a 10 day LC50s of 180 $ng.g^{-1}$ DW. It is known that this amphipod grows up to 10 mm and the average size of meiobenthic nematodes is about 1 mm which results in a biometric ratio of 10. For this reason, we decided to choose 18 $ng.g^{-1}$ DW as our maximum concentration (D3) after dividing the 10 day LC50s of 180 $ng.g^{-1}$ DW found for *Corophium volutator* by 10. Then, D1 and D2 were deduced after dividing D3 by 10 and 2, respectively. Thus, our D1 and D2 doses are moderately contaminated by ivermectin. However, D3, which has a higher ivermectin concentration, will correspond to the hypothetical sedimentary loads of ivermectin following its massive use as a COVID-19 treatment.

Experimental microcosms consisted of 2 L glass bottles. One liter of filtered lagoon water (0.1 μm) from the native site (37°09′10″N; 10°13′01″E) was used to fill the 12 microcosms since each of the four treatments was triplicated. All microcosms functioned as a closed system and received continuous ventilation via an air diffuser. The reliability of such an experimental design has been confirmed in numerous publications (Schratzberger and Warwick, 1998; Mahmoudi et al., 2005; Boufahja et al., 2015a, 2015b; Allouche et al., 2020b). After 10 days in darkness, the experiment ended and the sediment was preserved in 4% neutralized formaldehyde for further meiobenthic nematode study.

2.4. Nematode study

The extraction of meiofauna was performed using the levigation-decantation method followed by sieving on 1 mm and 40 μm sized mesh (Vitiello and Dinet, 1979). The meiofauna present in the sediment portion retained by the 40 μm sieve was kept in 4% formaldehyde and stained with a few drops of Rose Bengal (0.2 $g.l^{-1}$) until counting and identification began (Guo et al., 2001).

The meiofauna were tallied using a 50× stereomicroscope (Model WildHeerbrugg M5A) and 100 individuals were taken from each replicate. Microscopic slides were then prepared using the glycerol-ethanol rapid method as reported in Seinhorst (1959).

The identification of taxonomic and functional traits was performed using a 100× oil immersion objective attached to a Nikon DS-Fi2 camera and mounted on a Nikon microscope (Image Software NIS Elements Analysis Version 4.0 Nikon 4.00.07–build 787–64 bit). Genus identification required use of keys, specifically those of Platt and Warwick (1983, 1988) and Warwick et al. (1998). NeMys database

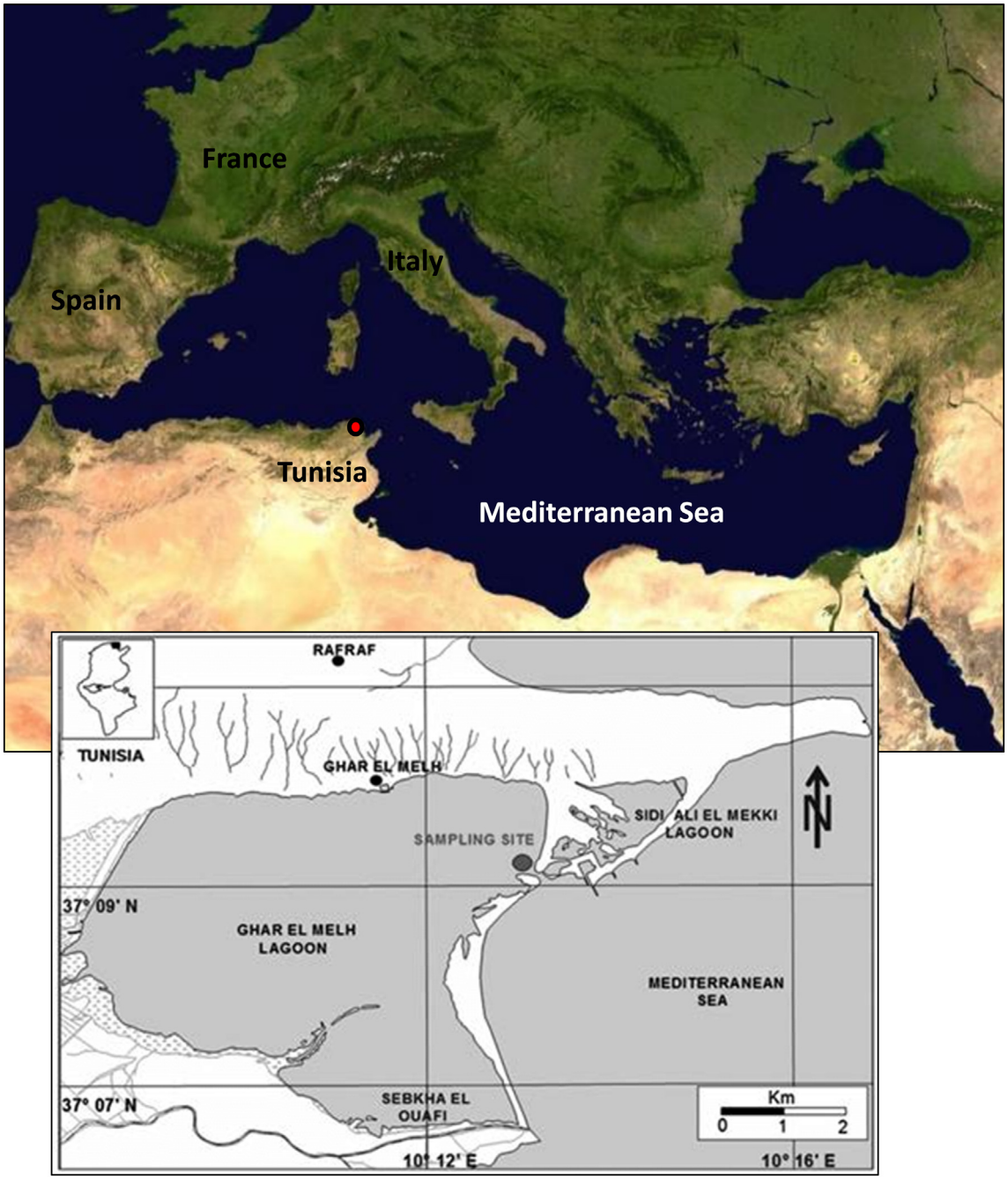

Fig. 1. Location of Ghar El Melh lagoon in relation to the Mediterranean Sea and the sampling site.

(Bezerra et al., 2019) was necessary to use in order to identify to species level after examination of the body features, measurement of several dimensions, and calculation of various morphometric ratios.

Nematode taxa were categorized into 4 types according to the morphological function of their buccal cavities (Wieser, 1953): selective deposit feeders (1A), non-selective deposit feeders (1B), epistrate-feeders (2A), and carnivores omnivores (2B). Additionally, the shape of the amphideal fovea was examined and five main categories were distinguished (Semprucci et al., 2018): indistinct (Id), pocket-like (Pk), spiral (Sp), rounded or elongated loop (REL), and circular (Cr).

2.5. Data processing

Statistical analyses of data were performed using the Plymouth Routines in Multivariate Ecological Research (Primer v5.0) software package via the standard methods described by Clarke (1993) and Clarke and Warwick (2001). For each microcosm, four univariate indices were considered: abundance, species number (S), Margalef's species richness (d), and Shannon index (H′, log_e). Two functional indices were considered: the Trophic Diversity Index (TDI) of Heip et al. (1985) and a new index we proposed, the Amphideal Diversity Index (ADI). The formula used for the calculation was identical, $\Sigma\boldsymbol{\theta}^2$, where $\boldsymbol{\theta}$ is the frequency of each functional category. High values indicate the predominance of one or more categories.

Data were first log_- or $log\,(x + 1)$-transformed to fulfill parametric requirements, Gaussian normality, and homogeneity of variances. Two tests were necessary: the Kolmogorov–Smirnov test to evaluate the first condition and the Bartlett to check the second condition. A one-way analysis of variance (AVOVA) was used to detect the overall significant difference between treatments. For multiple comparisons, the Tukey's

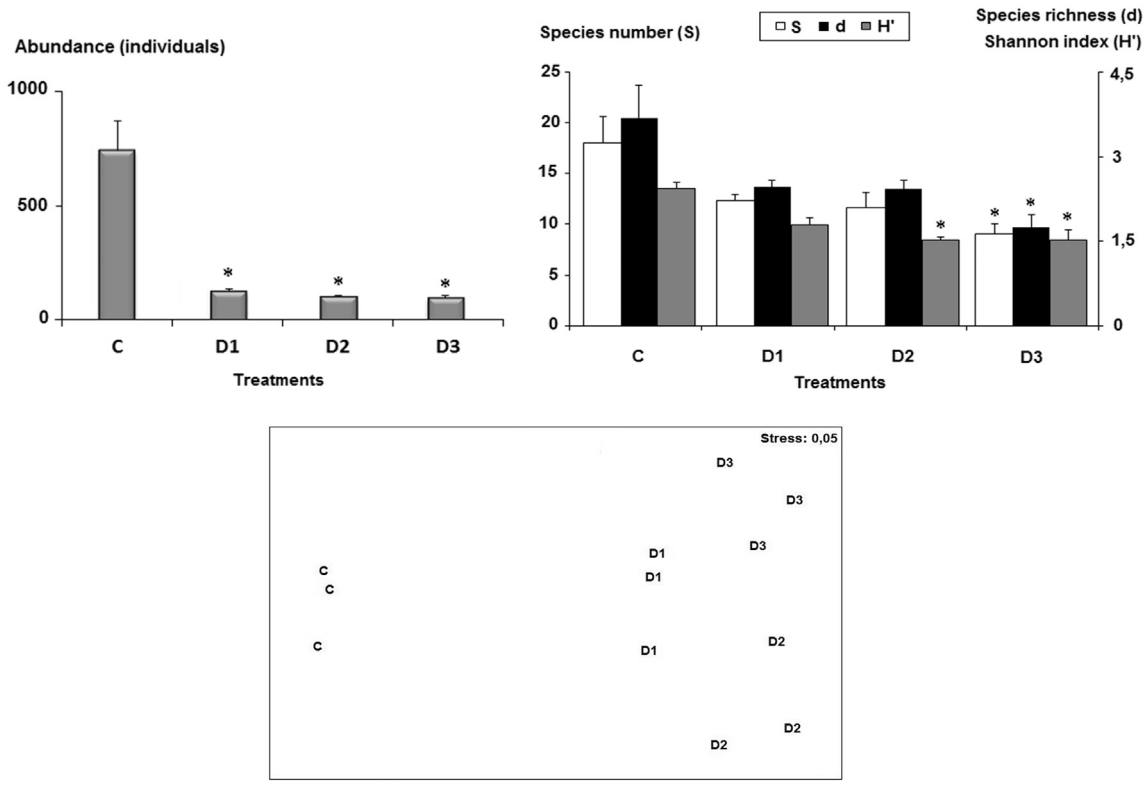

Fig. 2. Changes in abundance (above/left) and diversity indices (above/right) of meiobenthic nematodes for the control community (C) and following the addition of 3 concentrations of ivermectin (D1, D2, and D3) and the corresponding non-metric MDS plot based on species abundances (below). Asterisks above bars indicate significant differences ($p < 0.05$).

HSD test was used (Statistica version 5.1).

Three multivariate analyses were performed: (1) non-metric Multi-Dimensional Scaling ordination (nMDS) using the Bray-Curtis matrix of similarity, (2) Correspondence Analysis, and (3) the SIMPER procedure. The latter analysis was particularly useful for determining the contribution of each species or the mean functional trait dissimilarity with controls. The software PRIMER v5.0 was used to perform the first and third analyses and the software PAST v3.26 was used to perform the second analysis.

3. Results

3.1. Abundance

Ivermectin contamination caused a significant decrease in abundance and the community lost approximately ~6/7 of all individuals in terms of the average nematode abundance for all doses tested (Fig. 2). The results of our statistical analyses supported the pre-mentioned trend and the ivermectin replicates were significantly different from the controls but not from each other (Fig. 2).

3.2. Taxonomic diversity

Thirty-one species, belonging to 30 genera and 18 families, of meiobenthic nematodes were recorded in the control microcosms (C). The control community was dominated by four taxa with an average relative abundance higher than 10% each: *Paracomesoma dubium*, *Neochromadora poecilosomoides*, *Marylynnia stekhoveni*, and *Prochromadorella neapolitana* (Table 1).

The average values of species number and Margalef's Species Richness decreased corresponding to increased levels of ivermectin in the sediment. However, this pattern was only significant in the D3 dosage (Fig. 2). Regarding the Shannon Index, declines were also observed and significant declines began in the D2 dosage.

The ordination of microcosms by the nMDS method showed that ivermectin contamination had a clear effect on the taxonomic diversity of nematodes (stress = 0.05). Indeed, contaminated replicates are clearly separated from controls at the right side of the plot (Fig. 2). The SIMPER analysis showed an increase in the average taxonomic dissimilarity of control nematofauna with the increase of sedimentary ivermectin loads in relation with discernible changes in the abundance of several species (Table 2). Globally, the gradual addition of ivermectin to sediments was followed by two types of responses: (1) a lesser marked presence, if not a disappearance, of a first group of taxa which was composed of *Promonhystera* sp., *Bathylaimus australis*, *Chromadorita* sp., *Terschellingia longicaudata*, *N. poecilosomoides*, *Daptonema fallax*, *Theristus flevensis*, *Oncholaimus campylocercoides*, *Prochromadorella neapolitana*, and *Paramonohystera pilosa*; and (2) a higher presence of five species which include *Spirinnia gerlachi*, *Paracomesoma dubium*, *Marylynnia stekhoveni*, *Chromadorina metulata*, and *Microlaimus cyathlaimoides*.

3.3. Functional diversity

3.3.1. Feeding groups

The most abundant feeding categories of the control and ivermectin-contaminated microcosms were episterate feeders (2A) followed by non-selective deposit feeders (1B) (Fig. 3). The ordination of treatments using the nMDS method confirmed the significant trophic restructuring of the nematofauna after introducing ivermectin (stress = 0.09). Indeed, control replicates were separated from the ivermectin ones in the left side of the plot. Such treatment patterns were supported by an increase in average dissimilarity values of the controls corresponding with increasing ivermectin concentrations in the sediment (14.93–26.33%) (Table 2). This result was significantly accompanied by a greater presence of 2A nematodes and lesser presence of 1B

Table 1
Species list and biological traits of meiobenthic nematode species identified for the control community (C) and after addition of 3 concentrations of ivermectin (D1, D2 and D3). Feeding groups according to Wieser (1953) (FG): selective deposit-feeders (1A), non-selective deposit-feeders (1B), epistratum-feeders (2A), omnivores carnivores (2B); amphid shape (Am): circular (Cr); indistinct (Id); pocket-like (pk); rounded or elongate loop (REL); spiral (sp).

Species	Functional traits		Treatments			
	FG	Am	C	D1	D2	D3
Anticoma sp.	1A	Pk	1 ± 1		1.67 ± 1.53	
Axonolaimus sp.	1B	REL	0.33 ± 0.58			1 ± 1.73
Bathylaimus australis	1B	Sp	3 ± 0			
Chromadorita sp.	2A	Id	2.33 ± 1.53			
Chromadorina metulata	2A	Id	1.33 ± 1.53	4.67 ± 2.08	1.33 ± 1.53	
Chromadora nudicapitata	2A	Id	0.33 ± 0.58		0.67 ± 1.15	
Cyatholaimus prinzi	2A	SP	0.33 ± 0.58	0.67 ± 0.58	1 ± 0	
Daptonema normandicum	1B	Cr	0.33 ± 0.58		0.67 ± 1.15	
Daptonema fallax	1B	Cr	8.33 ± 2.08	8.67 ± 1.15		1.67 ± 0.58
Halalaimus gracilis	1A	REL	0.33 ± 0.58		0.67 ± 0.58	
Kraspedonema sp.	2A	Sp	0.33 ± 0.58		0.67 ± 1.15	1 ± 1
Marylynnia stekhoveni	2A	Sp	11.33 ± 1.15	18 ± 4.00	23.67 ± 8.33	16.67 ± 4.16
Microlaimus cyatholaimoides	2A	Cr	0.33 ± 0.58	1.33 ± 1.53	1.67 ± 1.53	6.33 ± 2.52
Metalinhomoeus numidicus	1B	Cr	1.33 ± 0.58	2.33 ± 0.58	2.67 ± 0.58	1.67 ± 0.58
Neochromadora poecilosomoides	2A	Id	12.67 ± 1.15	2.67 ± 1.53		1.67 ± 1.53
Nannolaimoides sp.	1A	Sp	0.33 ± 0.58			
Oncholaimus campylocercoides	2B	Pk	1.67 ± 0.58	0.33 ±		1 ± 1
Odontophora sp.	1B	REL	0.33 ± 0.58	0.67 ±	0.67 ± 0.58	1.33 ± 0.58
Paracomesoma dubium	2A	Sp	22 ± 4.58	43.67 ±	51.33 ± 7.23	40.67 ± 9.07
Paramonohystera pilosa	1B	Cr	8 ± 2	0.33 ± 0.58	1 ± 1	
Promonhystera sp.	1B	Cr	5.33 ± 1.53			
Prochromadorella neapolitana	2A	Id	10.67 ± 1.53	1.67 ± 2.08	0.67 ± 0.58	
Ptycholaimellus sp.	2A	Id	0.33 ± 0.58			
Spirinnia gerlachi	2A	REL	0.33 ± 0.58	11.33 ± 1.53	9.33 ± 3.21	27 ± 7
Synonchiella edax	2B	Sp	1 ± 1	0.33 ± 0.58	0.67 ± 1.15	
Siphonolaimus sp.	2B	Cr	0.33 ± 0.58	1 ± 1	0.67 ± 1.15	
Sphaerolaimus sp.	2B	Cr	0.33 ± 0.58			
Theristus flevensis	1B	Cr	3.67 ± 1.15	1.33 ± 1.15		
Terschellingia longicaudata	1A	Cr	1.33 ± 1.15		0.67 ± 0.58	
Thalassironus britannicus	2B	Pk	0.33 ± 0.58			
Viscosia sp.	2B	Pk	0.33 ± 0.58	1 ± 1.73	0.33 ± 0.5 8	

nematodes (Fig. 3, Table 2). The nematodes in groups 2B and 1A were particularly influenced by the lowest and highest concentrations of ivermectin, respectively (Table 2). The nMDS analyses based on distributions of species and feeding groups showed 87.28% of similarity.

3.3.2. Amphid shapes

The control community was dominated by taxa possessing spiral amphids, circular amphids, and indistinct amphids; those characterized by pocket-like or "rounded or elongated loop" amphids were less represented. The nMDS plot (Fig. 3, stress = 0.05) showed that the ivermectin contamination was followed by a discernible restructuring of the different categories of amphids. Indeed, the ivermectin treatments were placed far from controls in the nMDS plot (average dissimilarity with controls = 25.93–38.72%). On the other hand, the SIMPER analysis showed commonly significant numerical reduction for taxa with indistinct amphids and a stronger presence of those with "rounded or elongated loop" amphids. Occasional changes also occurred (1) at D1 where a higher abundance of nematodes with spiral amphids was observed, and (2) at D3 where a decrease in abundance was noted concerning nematodes with circular amphids. The nMDS analyses performed with species and amphids matrices showed 94.82% of similarity.

4. Discussion

Several studies have been published so far in association with the response of marine taxa after ivermectin exposure. Davies et al. (1997) reported a decrease in the abundance of the crustacean *Neomysis integer* as a result of a 10 day LC50 of 70 ng.l^{-1} ivermectin. In the case of the polychaete *Arenicola marina*, ivermectin toxicity was demonstrated in the laboratory and the 10-day LC50 was equal to 23 µg.kg^{-1} DW (Thain et al., 1997). For the amphipod *Corophium volutator* and the starfish *Asterias rubens*, the 10-day LC50s of ivermectin were much higher and corresponded to 0.18 mg.kg^{-1} DW and 23.6 mg.kg^{-1} DW, respectively (Davies et al., 1998). The crustacean *Daphnia magna* appeared to be more sensitive to ivermectin. Indeed, a significant reduction in the average abundance of this species was found in parallel with increasing ivermectin concentrations until a total disappearance was recorded at 1314 µg.kg^{-1} DW (Schweitzer et al., 2010). Boonstra et al. (2011) conducted an experiment to assess the effect of ivermectin on zooplankton and macroinvertebrates. For zooplanktonic organisms, authors reported a reduction in abundance for two cladoceran species (*Chydorus sphaericus* and *Daphnia longispinas*). Similar results were previously found by Sanderson et al. (2007) who reported that cladocerans completely disappear from ivermectin-contaminated microcosms following 10 days of contamination at a concentration of 30 ng.l^{-1}. In the case of macroinvertebrates, Boonstra et al. (2011) reported that 27 days of exposure to 1 µg.l^{-1} of ivermectin resulted in a significant decrease in density of the amphipod *Gammarus pulex*. Although these results are interesting, they remain local as the studied taxa have restricted geographical distributions which are not appropriate in the case of globally widespread COVID-19. In contrast, the results obtained in this study could be universally generalized since (1) nematodes are the most abundant and diversified biota in marine areas (Boufahja et al., 2015b); (2) they are known to be ubiquitous and are often the last organisms to disappear in extreme conditions (Heip et al., 1985); and (3) species are cosmopolitan, which is classically known as the "meiofauna paradox" (Boeckner et al., 2009).

The current study confirmed that features of meiobenthic nematodes have been significantly affected by the sedimentary ivermectin enrichment. This effect was deduced from a significant reduction of both abundance and diversity descriptors. Particularly, the highest dose

Table 2
Dissimilarity percentages (Av. Diss) between the control community (C) and those exposed to ivermectin (D1, D2 and D3) and results of SIMPER analysis. Only species and functional traits accounting for ~70% of overall dissimilarity are given. More abundant (+); less abundant (−); eliminated (ø); feeding group (FG); selective deposit-feeders (1A), non-selective deposit-feeders (1B), epistratum-feeders (2A), omnivores carnivores (2B); amphid shape (Am); circular (Cr); indistinct (Id); rounded or elongate loop (REL); spiral (sp).

	Species	Functional traits	
		FG	Am
C vs. D1	**Av. Diss = 45.13%**	**Av. Diss = 14.93%**	**Av. Diss = 25.93%**
	Spirinnia gerlachi 9.92% (+)	1B 40.81% (−)	REL 35.24% (+)
	Paramonohystera pilosa 8.12% (−)	2A 25.68% (+)	Id 23.05% (−)
	Promonhystera sp. 7.53% (ø)	2B 18.21% (−)	Sp 15.99% (+)
	Prochromadorella neapolitana 7.39% (−)		
	Neochromadora poecilosomoides 6.52% (−)		
	Paracomesoma dubium 6.27% (+)		
	Bathylaimus australis 5.67% (ø)		
	Chromadorita sp. 4.84% (ø)		
	Chromadorina metulata 3.92% (+)		
	Theristus flevensis 3.15% (−)		
	Oncholaimus campylocercoides 3.10% (−)		
	Terschellingia longicaudata 3.03% (ø)		
	Marylynnia stekhoveni 2.84% (+)		
C vs. D2	**Av. Diss = 56.42%**	**Av. Diss = 21.05%**	**Av. Diss = 36.15%**
	Neochromadora poecilosomoides 9.63% (ø)	1B 51.53% (−)	Id 28.67% (−)
	Daptonema fallax 7.75% (ø)	2A 23.72% (+)	REL 24.79% (+)
	Spirinnia gerlachi 7.28% (+)		Cr 20.70% (−)
	Prochromadorella neapolitana 7% (−)		
	Paracomesoma dubium 6.68% (+)		
	Promonhystera sp. 6.22% (ø)		
	Paramonohystera pilosa 5.42% (−)		
	Theristus flevensis 5.16% (ø)		
	Bathylaimus australis 4.69% (ø)		
	Chromadorita sp. 4% (ø)		
	Marylynnia stekhoveni 3.93% (+)		
	Oncholaimus campylocercoides 3.45% (ø)		
C vs. D3	**Av. Diss = 57.65%**	**Av. Diss = 26.33%**	**Av. Diss = 38.72%**
	Spirinnia gerlachi 13.16% (+)	1B 45.24% (−)	REL 37.30% (+)
	Prochromadorella neapolitana 8.88% (−)	2A 22.71% (+)	Id 29.59% (−)
	Paramonohystera pilosa 7.66% (−)	1A 19.62% (ø)	Cr 16.27% (−)
	Neochromadora poecilosomoides 6.89% (ø)		
	Promonhystera sp. 6.27% (ø)		
	Microlaimus cyatholaimoides 5.87% (+)		
	Theristus flevensis 5.20% (ø)		
	Bathylaimus australis 4.72% (ø)		
	Paracomesoma dubium 4.58% (+)		
	Daptonema fallax 4.33% (ø)		
	Chromadorita sp. 4.03% (ø)		

D3 caused a significant negative effect for all univariate indices considered. Several qualitative changes were detected through multivariate analyses beginning with the lowest ivermectin concentration administrated in reference to the controls. The Correspondence Analysis summarized all the nematode responses and described the shift in taxonomic and functional traits of the nematofauna in ivermectin-contaminated sediments (Fig. 4).

The results of the SIMPER analysis (Table 2) and those shown in the Correspondence Analysis plot (Fig. 4) confirmed that the presence of ivermectin was harmful to 13 nematode species, considered herein as negative bioindicators, namely, *Promonhystera* sp., *Bathylaimus australis*, *Chromadorita* sp., *Terschellingia longicaudata*, *N. poecilosomoides*, *Daptonema fallax*, *Theristus flevensis*, *Oncholaimus campylocercoides*, *Prochromadorella neapolitana*, *Paramonohystera pilosa*, *Synonchiella edax*, *Sphaerolaimus* sp., and *Thalassironus britannicus*. The life styles and niches abounded by these sensitive species after ivermectin exposure were obviously occupied by 12 positive bioindicative taxa which, in contrast, appeared to be opportunistic: *Spirinnia gerlachi*, *Microlaimus cyathlaimoides*, *Kraspedonema* sp., *Odontophora* sp., *Paracomesoma dubium*, *Marylynnia stekhoveni*, *Metalinhomoeus numidicus*, *Chromadorina metulata*, *Cyatholaimus prinzi*, *Chromadora nudicapitata*, *Halalaimus gracilis*, and *Siphonolaimus* sp.

The responses of the aforementioned nematode taxa to sediment ivermectin enrichment were dependent on their functional features and more intensely to their amphid shape. In detail, species belonging to the functional type 1B-Cr-Id were disadvantaged for the benefit of the functional type 2A-REL-Sp. This explains why the Trophic Diversity Index and Amphideal Diversity Index increased with increasing ivermectin concentrations in the sediment. It is known that amphids likely play a role in nematode chemoreception (Decraemer et al., 2014; Cesaroni et al., 2017). Logically, a larger amphid could be more efficient in detecting xenobiotics like ivermectin in the surrounding environment. The small sizes of the circular amphids of non-selective deposit feeders or indistinct amphids of Chromadorids did not allow those taxa to detect and avoid ivermectin. Such a handicap may explain the massive mortality observed in the nematode functional type 1B-Cr-Id. As result, contaminated sediments should be enriched with dead bodies which will be beneficial in the creation of new micro-habitats and ecological niches. The nematodes belonging to the functional type 2A-REL-Sp seem to be more adapted to this type of sediment since their "rounded or elongated loop" and spiral amphids are large and theoretically allow efficient detection and avoidance of ivermectin. This functional type was characterized as opportunistic species since, after hiding in microhabitats organically enriched with decomposing bodies, they will survive by consuming diatoms and ciliates. These latter taxa are known to be advantaged by the organic enrichment of the

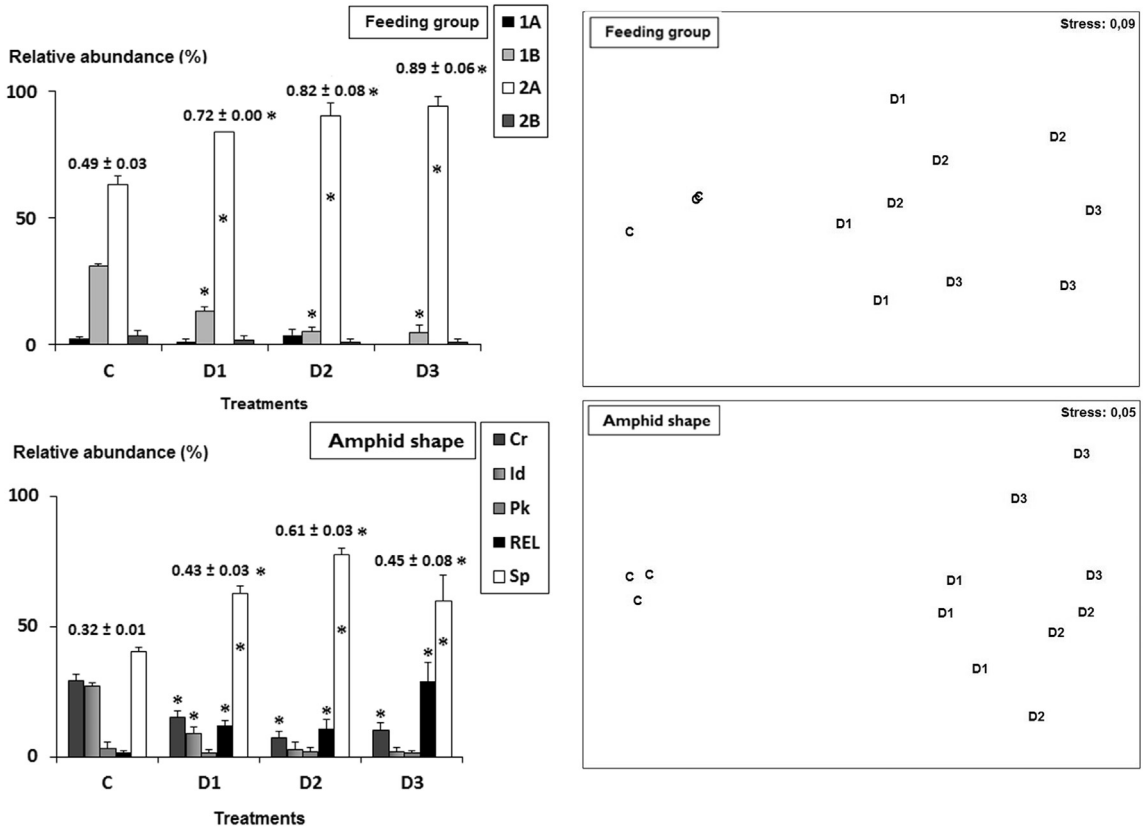

Fig. 3. Graphical summary (left) and non-metric multidimensional scaling (nMDS) 2D plots (right) based on the abundance nematode functional groups for the control community (C) and following the addition of 3 concentrations of ivermectin (D1, D2, and D3). Selective deposit feeders (1A); non-selective deposit feeders (1B); epistrate feeders (2A); omnivores-carnivores (2B); circular (Cr); indistinct (Id); pocket-like (pk); rounded or elongated loop (REL); spiral (sp). Values (± SD) above bars indicate the Trophic Diversity Index (upper values) and Amphideal Diversity Index (lower values). Asterisks above bars indicate significant differences ($p < 0.05$).

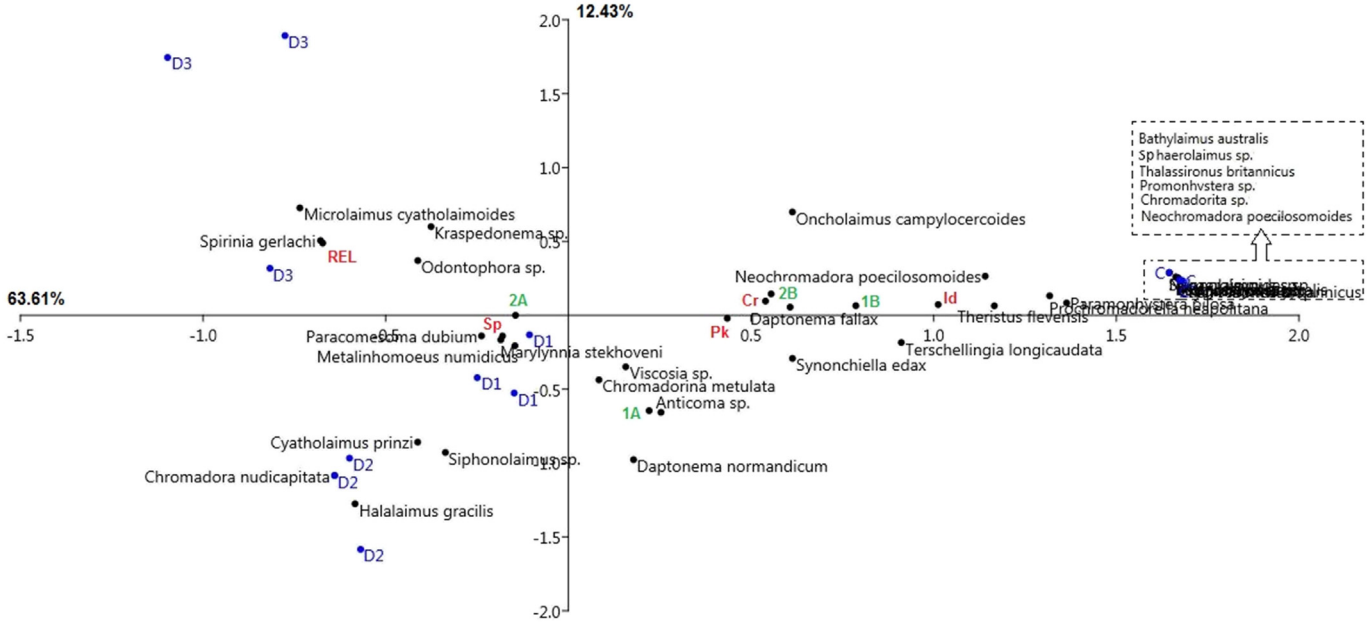

Fig. 4. Correspondence Analysis (CA) 2D plot based on the abundance of nematode species and functional groups for the control community (C) and following the addition of 3 concentrations of ivermectin (D1, D2, and D3). Selective deposit feeders (1A); non-selective deposit feeders (1B); epistrate feeders (2A); omnivores-carnivores (2B); circular (Cr); indistinct (Id); pocket-like (pk); rounded or elongated loop (REL); spiral (sp).

environment (Boucher, 1997; Raes et al., 2007). On the other hand, it seems that the mortality of sensitive taxa occurred at the start of the experiment. This was assumed since the frequency of predators was low at the end which means that freshly dead prey were rare (Moens and Vincx, 1997; Semprucci et al., 2018). Alternatively, nematodes belonging to the functional type 2A-REL-Sp may eventually develop detoxification mechanisms to tolerate bodily exposure to ivermectin (Allouche et al., 2020c). As a result of anticipated rigorous usage of ivermectin during the COVID-19 pandemic, fishes and other macrobenthic groups (e.g., crab, lobster, shrimp, and prawn) may easily accumulate this drug due their higher ranking in the marine food chain as well as their consumption of nematodes during juvenile stages (Wilcox and Jeffries, 1979; Albertini-Berhaut, 1974; Fitzhugh and Fleeger, 1985). Thus, the safety of seafoods for human consumption should be cautiously monitored, as these organisms will contain high amounts of ivermectin, especially if they are captured near the coasts of countries severely impacted by the COVID-19 pandemic.

5. Conclusions

Ivermectin has long been used as an anti-parasitic treatment. Lately, this chemical has been proposed to be an effective and quick remedy for COVID-19 (Caly et al., 2020). In case ivermectin is extensively utilized to suppress the spread of COVID-19, we predict that high quantities of ivermectin will be deposited into the sea. We are particularly concerned about potential contamination of the Mediterranean Sea since (1) it is a semi-closed ecosystem characterized by a low renewal rate of its waters, and (2) due the fact that three surrounding countries have experienced very high COVID-19 infection and death rates, namely, Italy, Spain, and France. We decided to use meiobenthic nematodes to determine whether ivermectin could be safely used as a quick and extensive treatment against COVID-19 and our results were supported by their ubiquism, and cosmopolitan species behaviour. Therefore, the results obtained from the examined nematode community, collected in Tunisia, could be valid all over the world. Our results confirmed that the presence of ivermectin was ecotoxic for meiobenthic nematodes after causing a significant reduction in abundance and taxonomic diversity. The functional type that was revealed to contain the most ivermectin was composed of nematodes 2A-REL-Sp which could be indicative of unsafe seafoods.

Declaration of competing interest

The authors declare that they have no known competing financial interests or personal relationships that could have appeared to influence the work reported in this paper.

Acknowledgements

The authors extend their appreciation to the Deanship of Scientific Research at King Saud University for funding the Research group RG-254 and to RSSU at King Saud University for their technical support.

References

Abd El-Aziz, T.M., Stockand, J.D., 2020. Recent progress and challenges in drug development against COVID-19 coronavirus (SARS-CoV-2) – an update on the status. Infect. Genet. Evol. 83, 104327.

Albertini-Berhaut, J., 1974. Biologie des stades juvéniles des Téléostéens Mugilidae *Mugil auratus* R 1810 *Mugil capito* C 1829 et *Mugil saliens* R 1810. II. Modification du régime alimentaire en relation avec la taille. Aquaculture 4, 13–27.

Allouche, M., Nasri, A., Harrath, A.H., Mansour, L., Beyrem, H., Boufahja, F., 2020a. Migratory behavior of free-living marine nematodes surrounded by sediments experimentally contaminated by mixtures of polycyclic aromatic hydrocarbons. J. J. King Saud Univ. Sci. 32, 1339–1345.

Allouche, M., Hamdi, I., Nasri, A., Harrath, A.H., Mansour, L., Beyrem, H., Boufahja, F., 2020b. Laboratory bioassay exploring the effects of anti-aging skincare products on free-living marine nematodes: a case study of collagen. Environ. Sci. Pollut. Res. 27, 11403–11412.

Allouche, M., Nasri, A., Harrath, A.H., Mansour, L., Alwasel, S., Beyrem, H., Bourioug, M., Geret, F., Boufahja, F., 2020c. New protocols for the selection and rearing of *Metoncholaimus pristiurus* and the first evaluation of oxidative stress biomarkers in meiobenthic nematodes. Envon. Pollut. 263 (B), 114529.

Beyrem, H., Mahmoudi, E., Essid, N., Hedfi, A., Boufahja, F., Aïssa, P., 2007. Individual and combined effects of cadmium and diesel on a nematode community in a laboratory microcosm experiment. Ecotoxicol. Environ. Saf. 68, 412–418.

Beyrem, H., Louati, H., Essid, N., Aïssa, P., Mahmoudi, E., 2010. Effects of two lubricant oils on marine nematode assemblages in a laboratory microcosm experiment. Mar. Environ. Res. 69, 248–253.

Bezerra, T.N., Decraemer, W., Eisendle-Flöckner, U., Hodda, M., Holovachov, O., Leduc, D., Miljutin, D., Mokievsky, V., Peña Santiago, R., Sharma, J., Smol, N., Tchesunov, A., Venekey, V., Zeng, Z., Vanreusel, A., 2019. In: Bezerra, T.N. (Ed.), NeMys: World Database of Nematodes. Ghent University available at. http://nemys.ugent.be/.

Boeckner, M.J., Sharma, J., Proctor, H.C., 2009. Revisiting the meiofauna paradox: dispersal and colonization of nematodes and other meiofaunal organisms in low- and high-energy environments. Hydrobiologia 624, 91–106.

Boonstra, H., Reichman, E.P., Van den Brink, P.J., 2011. Effect oft he veterinary pharmaceutical ivermectin in indoor aquatic microcosms. Arch. Environ. Contam. Toxicol. 60 (1), 77–89.

Boucher, G., 1997. Structure and biodiversity of nematode assemblages in the SW lagoon of New Caledonia. Coral Reefs 16, 177–186.

Boufahja, F., Ismaïly, S., Beyrem, H., 2015a. Experimental evidence of effects of an antimitotic agent, colchicine, on a nematode community through a microcosm approach. Cah. Biol. Mar. 56, 39–48.

Boufahja, F., Semprucci, F., Beyrem, H., Bhadury, P., 2015b. Marine nematode taxonomy in Africa: promising prospects against scarcity of information. J. Nematol. 47 (3), 1–9.

Buchanan, J.B., 1971. Measurement of the physical and chemical environment: sediments. In: Holme, N.A., McIntyre, A.D. (Eds.), Methods for the Study of Marine Benthos. International Biological Programme Handbook No. 16. Blackwell Scientific Publications, Oxford (334 pp).

Caly, L., Druce, J.D., Catton, M.G., Jans, D.A., Wagstaff, K.M., 2020. The FDA-approved drug ivermectin inhibits the replication of SARS-1 CoV-2 *in vitro*. Antivir. Res. 178, 104787.

Cesaroni, L., Guidi, L., Balsamo, M., Semprucci, F., 2017. Scanning electron microscopy in the taxonomical study of free-living marine nematodes. Microscopie 31–38.

Clarke, K.R., 1993. Non-parametric multivariate analyses of changes in community structure. Aust. J. Ecol. 18, 117–143.

Clarke, K.R., Warwick, R.M., 2001. Changes in Marine Communities: An Approach to Statistical Analysis and Interpretation, 2nd edition. PRIMER-E, Polymouth., UK (164 p).

Coull, B.C., Chandler, G.T., 1992. Pollution and meiofauna: field, laboratory and mesocosm studies. Oceanogr. Mar. Biol. 30, 191–271.

Davies, I.M., McHenery, J.G., Rae, G.H., 1997. Environmental risk from dissolved ivermectin to marine organisms. Aquaculture 158, 263–275.

Davies, I.M., Gillibrand, P.A., McHenery, J.G., Rae, G.H., 1998. Environmental risk of ivermectin to sediment dwelling organisms. Aquaculture 163 (1–2), 29–46.

Decraemer, W., Coomans, A., Baldwin, J., 2014. Morphology of nematoda. In: Schmidt-Rhaesa (Ed.), Handbook of Zoology, Gastrotricha, Cycloneuralia and Gnathifera. De Gruyter, Berlin, pp. 1–51.

Fabiano, M., Danovaro, R., 1994. Composition of organic matter in sediment facing a river estuary (Tyrrhenian Sea): relationships with bacteria and microphytobenthic biomass. Hydrobiologia 277, 71–84.

Fitzhugh, G.R., Fleeger, J.W., 1985. Goby (Pisces: Gobiidae) interactions with meiofauna and small macrofauna. Bull. Mar. Sci. 36 (3), 436–444.

Guo, Y., Somerfield, P.J., Warwick, R.M., Zhang, Z., 2001. Large-scale patterns in the community structure and biodiversity of free living nematodes in the Bohai Sea. China. J. Mar. Biol. Assoc. UK 81, 755–763.

Halley, B.A., van den Heuvel, W.J.A., Wislocki, P.G., 1993. Environmental effects of the usage of avermectins in livestock. Vet. Parasitol. 48, 109–125.

Hedfi, A., Mahmoudi, E., Boufahja, F., Beyrem, H., Aïssa, P., 2007. Effects of increasing levels of nickel contamination on structure of offshore nematode communities in experimental microcosms. Bull. Environ. Contam. Toxicol. 79, 345–349.

Heip, C., Vincx, M., Vranken, G., 1985. The ecology of marine nematodes. Oceanogr. Mar. Biol. 23, 399–489.

Hermi, H., Mahmoudi, E., Beyrem, H., Aïssa, P., Essid, N., 2009. Responses of a free-living marine nematode community to mercury contamination: results from microcosm experiments. Arch. Environ. Contam. Toxicol. 56, 426–433.

Lee, M.R., Correa, J.A., 2005. The effects of copper mine tailings disposal on littoral meiofaunal assemblages in the Atacama region of northern Chile. Mar. Environ. Res. 59, 1–18.

Louati, H., Ben Said, O., Got, P., Soltani, A., Mahmoudi, E., Cravo-Laureau, C., Duran, R., Aïssa, P., Pringault, O., 2013. Microbial community responses to bioremediation treatments for the mitigation of low-dose anthracene in marine coastal sediments of Bizerte lagoon (Tunisia). Environ. Sci. Pollut. Res. 20 (1), 300–310.

Mahmoudi, E., Essid, N., Beyrem, H., Hedfi, A., Boufahja, F., Vitiello, P., Aïssa, P., 2005. Effects of hydrocarbon contamination on a free-living marine nematode community: results from microcosm experiments. Mar. Pollut. Bull. 50, 1197–1204.

Mahmoudi, E., Essid, E., Beyrem, H., Hedfi, A., Boufahja, F., Vitiello, P., Aïssa, P., 2007. Individual and combined effects of lead and zinc of a free living marine nematode community: results from microcosm experiments. J. Exp. Mar. Biol. Ecol. 343, 217–226.

Mesa, L., Gutiérrez, M.F., Montalto, L., Perez, V., Lifschitz, A., 2020. Concentration and environmental fate of ivermectin in floodplain wetlands: an ecosystem approach. Sci.

Total Environ. 706, 135692.
Moens, T., Vincx, M., 1997. Observations on the feeding ecology of estuarine nematodes. J. Mar. Biol. Assoc. UK 77, 211–227.
Platt, H.M., Warwick, R.M., 1983. Free living marine nematodes. In: Part I. British Enoplids. Synopses of the British Fauna no 28. Cambridge University Press, Cambridge (314 p).
Platt, H.M., Warwick, R.M., 1988. Free living marine nematodes. In: Part II. British Chromadorids. Synopses of the British Fauna no 38. E.J Brill, Leiden (502 p).
Raes, M., De Troch, M., Ndaro, S.G.M., Muthumbi, A., Guilini, K., Vanreusel, A., 2007. The structuring role of microhabitat type in coral degradation zones: a case study with marine nematodes from Kenya and Zanzibar. Coral Reefs 26, 113–126.
Sanderson, H., Laird, B., Pope, L., Brain, R., Wilson, C., Johnson, D., Bryning, G., Peregrine, A.S., Boxall, A., Solomon, k., 2007. Assessment of the environmental fate and effects of ivermectin in aquatic mesocosms. Aquat. Toxicol. 85, 229–240.
Schratzberger, M., Warwick, R.M., 1998. Effects of intensity and frequency of organic enrichment on two estuarine nematode communities. Mar. Ecol. Prog. Ser. 164, 83–94.
Schratzberger, M., Whomersley, P., Warr, K., Bolam, S.G., Rees, H.L., 2004. Colonisation of various types of sediment by estuarine nematodes *via* lateral infaunal migration: a laboratory study. Mar. Biol. 145, 69–78.
Schweitzer, N., Fink, G., Ternes, T.A., Duis, K., 2010. Effects of ivermectin-spiked cattle dung on a water-sediment system with the aquatic invertebrates *Daphnia magna* and *Chironomus riparius*. Aquat. Toxicol. 97, 304–313.
Seinhorst, J.W., 1959. A rapid method for the transfer of nematodes from fixative to anhydrous glycerin. Nematologica 4, 67–69.
Semprucci, F., Cesaroni, L., Guidi, L., Balsamo, M., 2018. Do the morphological and functional traits of free-living marine nematodes mirror taxonomicalal diversity? Mar. Environ. Res. 135, 114–122.
Thain, J.E., Davies, I.M., Rae, G.E., Allen, Y.T., 1997. Acute toxicity of ivermectin to the lugworm *Arenicola marina*. Aquaculture 159 (1–2), 47–52.
Vitiello, P., Dinet, A., 1979. Définition et échantillonnage du méiobenthos. Rapp. Comm. Int. Expl. Sci. Mer. Médit. 25, 279–283.
Warwick, R.M., Platt, H.M., Somerfield, P.J., 1998. Free-living marine nematodes. In: Part III. British Monohysterids. Synopsis of British Fauna (New Series) No. 53. Field Studies Council, Shrewsbury.
Whitworth, J., 2020. COVID-19: a fast evolving pandemic. Trans. R. Soc. Trop. Med. Hyg. 114 (4), 241–248.
Wieser, 1953. Die Beziehung zwischen Mundhoehlengestalt, Ernaehrugsweise und Vorkommen bei freilebenden marinen Nematoden. Arkiv. Fur. Zoologi. 4, 439–484.
Wilcox, J.R., Jeffries, H.P., 1979. Feeding habits of the sand shrimp *Crangon septemspinosa*. Biol. Bull. 146, 424–434.